

**The Effect of Laser-Induced Micro Grooving on Cemented Total Knee
Replacement**

Sama Desmond Nuyebga

Master of Science in Engineering Physics-Mechanical Engineering

University of Central Oklahoma

Edmond, Oklahoma

May, 2019

Master Thesis

Submitted to the Faculty of

the Graduate collage of the University of Central Oklahoma

in partial fulfillment of the requirements for Degree of

Master of Science

May 2019

The Effect of Laser-Induced Micro Grooving on Cemented Total Knee Replacement

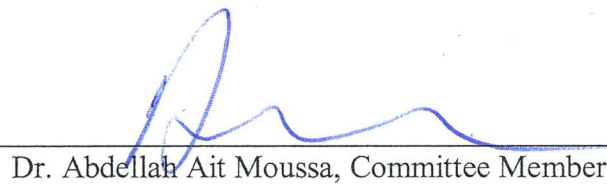
Thesis Approved:



Dr. Morshed Khandaker, Committee Chair



Dr. Weldon Wilson, Committee Member



Dr. Abdellah Ait Moussa, Committee Member

Acknowledgement

I am most grateful to God the father almighty for giving me a wonderful supervisor Dr Morshed Khanderka who was always present to provide continuous support, motivation, enthusiasm, and transfer of knowledge in this study. Dr Khandaker provided self-less service, working during weekends and being available at all times to respond to all my worries and problems.

My appreciation goes to Dr. Weldon Wilson and Dr. Dr. Abdellah Ait Moussa for their encouragement and support during my research. Dr Wilson was always available on call at all times acting as my advisor. Dr Moussa provided me with other special equipment necessary for this project. He also provided me with on the spot training to use those equipment.

Finally, my sincere gratitude goes to my wife Nahbila Lysette for being there for me and to my family; mother Jocelyn, father Pryde, Brothers; Eugene, Primus and Arnold and to my one and only sister Hilda.

Abstract

Total knee replacement implant surgery is at an all-time high, with 10% of Americans age 80 and older are currently living with at least one total knee replacement (TKR). An ideal implant should ensure lifelong mechanical stability with the adjoining tissues. However, micromotions that occur at the implant surface activate osteoclasts, which resorb bone around the implant and contribute to implant loosening and eventual implant failure. A method to improve mechanical fixation of a TKR implant is clinically important and is the purpose of the proposed research project. This research uses a noble method that designs microgrooves on tibia tray using a laser. The goal of this study is to measure the effects of the designed microgrooves on a tibia implant that is used in dogs. The first objective of this study was to design a tibia tray for a dog by using a 3-D scanner and exporting the image into solid works. Solid works was used to design the tibia and CNC machine was used to machine the part. Six samples were made, and laser machine was used to produce laser microgrooves on three of the samples. The samples were characterized by measuring the roughness. The second objective was to design the experimental setup for use in Test Resource machine to measure the effects of grooves on the fatigue life. The third objective was to perform finite element analysis on the groove and the non-groove tibia tray and compare the results with the test result. The results were analyzed after 100000 cycles and data showed that there was a 0.017 increase in the stroke from the initial stroke to the final stroke. Using an X-ray imaging technique with a dental X-ray camera, there were some traces of cracks indicating there was a micromotion between the implant and bone. The samples with Microgrooves showed significant stability from the samples with no grooves.

Table of Contents

Acknowledgement	iii
Abstract	iv
List of figures	vii
Chapter 1 Introduction.....	1
1.1. Total Knee Replacement.....	1
1.2. Reasons for Total Knee Replacement Surgery	3
1.3. Total Knee replacement Material	4
1.4. Problem Statement	6
1.5. Hypothesis.....	7
1.6. Motivation and Goals	7
1.7. Objectives	8
1.8. Organization of the thesis	8
Chapter 2 Tibia Tray Design Using Solid Works, Manufacture Using CNC Machine and Characterization Using a Profiler.	10
2.1. Abstract.....	10
2.2. Introduction.....	10
2.3. Summary.....	11
2.4. Materials and Methods	11
2.5. Results.....	15

2.6.	Conclusion	18
Chapter 3	Experimental study to evaluate the effect of groove on static and cyclic load. ...	20
3.1.	Abstract.....	20
3.2.	Introduction.....	21
3.3.	Materials and Method.....	21
3.4.	Design of Experiment.....	28
3.5.	Results.....	31
3.6.	Conclusion	36
Chapter 4	Finite element analysis to evaluate the stress distribution around tibia tray implant due to static and cyclic load	37
4.1.	Abstract.....	37
4.2.	Introduction.....	37
4.3.	Method.....	38
4.4.	Results and Discussion.....	41
4.5.	Comparison of DIC Strain and FEA Strain	44
4.6.	Conclusion	45
Chapter 5	Conclusion and future work.....	46
5.1.	Conclusion	46
5.2.	Future Work.....	47
	References	48

List of figures

Figure 1-1: Total knee replacement surgery with femoral and tibia tray(https://www.mayoclinic.org).....	3
Figure 1-2: PMMA bone cement used in the study; Biomedtrix 3 Veterinarian bone cement	6
Figure 2-1: Open-frame desktop 3D scanners	13
Figure 2-2: Scanned image of a dog tibia	13
Figure 2-3: Design of a tibia tray on scan tibia-fibula. (a) Model with microgrooves. (b) Model with no grooves.	14
Figure 0-4: Image of the tibia tray ready for machining. (a) Smooth tibia tray. (b) Tibia tray with Microgrooves.....	14
Figure 2-5: Machine data	15
Figure 2-6: Tibia tray machined in CNC machine	16
Figure 0-7: profiler image of smooth sample roughness.	17
Figure 2-8: Details of roughness of smooth tibia tray	17
Figure 2-9: Tibia tray with Micro grooves.....	17
Figure 2-10: Profiler image of tibia with grooves	18
Figure 2-11: Details of mean roughness of tibia tray with grooves.....	18
Figure 3-1: Part (a) with a point attachment to the compression machine.....	22
Figure 3-2: Experimental part (b)	22
Figure 3-3: Bottom part, part (c).	23
Figure 3-4: Experimental setup design	23

Figure 3-5: Test tools designed and ready for assembly onto test resources for experiment.	24
Figure 3-6: the process of cutting the sawbone	24
Figure 3-7: six saw bones cut according to surgical procedure.....	25
Figure 3-8: tibia fibula bone with a hole to accommodate tibia tray.	25
Figure 3-9: Preparation of 2.40g of PMM cement.....	26
Figure 3-10: Fixation of implant into the bone	27
Figure 3-11: mounting of the sample on compression test machine	28
Figure 3-12: complete setup of the system for fatigue test	29
Figure 3-13: Details of fatigue test	30
Figure 3-14: changes in the amplitude of oscillation as a result of fatigue test.	31
Figure 3-15: X-ray images before and after fatigue test. (a) before fatigue test (b) after fatigue test	32
Figure 3-16: X-ray images grooved sample before and after fatigue test. (a) before fatigue test (b) after fatigue test.....	33
Figure 3-17: A graph of load vs stroke to indicate the point of failure for tibia tray without grooves	34
Figure 3-18: A graph of load vs stroke to show the changes in tibia tray with grooves	35
Figure 4-1: Fine meshing	39
Figure 4-2: Bonded contacts between bone and tibia tray	40
Figure 4-3: Deformation characteristics of top view of cemented tibia tray on bone	41
Figure 0-7: Side view of cemented tibia tray	42
Figure 4-5: Variation of displacement per node	42

Figure 4-6: a graph of Load against deformation43

Chapter 1 Introduction

1.1. Total Knee Replacement

Science has helped improve living standards and healthy living, however the need for a perfectly functioning knee replacement is at an all-time high, where 10% of Americans at the age 80 and above are currently living having at least one total knee replacement (TKR) [1]. Statistics reported that, as of 2012, 4.5 million Americans were living with at least one total knee replacement; this in turn accounts for roughly 4.7% of the population age 50 years or older [2]. These statistics indicate the necessity for this type of important procedure, as the knee is heavily influential in the dynamic mobility of the human body. Without a functioning knee, a patient is extremely confined, with hindered movement causing a devastating loss of mobility.

In addition, with the average lifespan increasing, the need for treatment which preserves and restores normal body functionality is becoming much more in demand. Approximately 90% of the total number of total knee replacement surgeries performed has occurred within the last 10 years [3], a clear indication of how this surgical operation has increasingly become a seemingly routine orthopedic procedure to remedy the immobility associated with a malfunctioning knee. Subsequently, the demand for a successful method of restoration of the knee is at an all-time high, which is why total knee replacement surgery is currently so popular.

Additionally, the popularity of this surgery is reflected in the statistics; for instance, 95% of patients report that they are satisfied with their procedure [3]. This procedure is sustainable as well, as the revision rate is fairly low. In another study, it was found that

revision rates of 12% after 10 years are common in the United States [4]. The typical reason for revision after a long time period such as 10 years is due to loosening of the implant and general wear due to dynamic fatigue. This type of surgery also has a very low complication rate. Based on a study of 1.82 million patient records in all age groups, 7.5% of patients endure complications within 90 days of surgery [4]. These comprehensive statistics indicate the demand, and the effectiveness of total knee replacement surgery, which has truly become a growing industry within the medical community.

Total knee replacement surgery is a procedure whereby part of the knee joint is replaced with artificial material [3]. The artificial material usually titanium is held in position using a cement. The cemented total joint prosthesis is one of the most frequent operations in the orthopedic fields. Poly methyl methacrylate (PMMA) bone cements are widely used to fix artificial joints for filling the free space between bone and prostheses.

The biggest challenge in knee surgery and orthopedic research are the implant loosening at the interface or the breakage at the point of implantation [5]. The mechanical failure of the implant-cement interfaces has been proposed as one of the most possible causes leading to the eventual clinical loosening of cemented total joint prosthesis. It is an active area of research to develop an optimal implant-cement interface by improving mechanical stability of PMMA bone cement. PMMA bone cement, which are used in human and animal orthopedics surgeries, show fast and slow curing properties.

A total knee replacement is shown in Figure 1-1 with all the parts clearly shown.

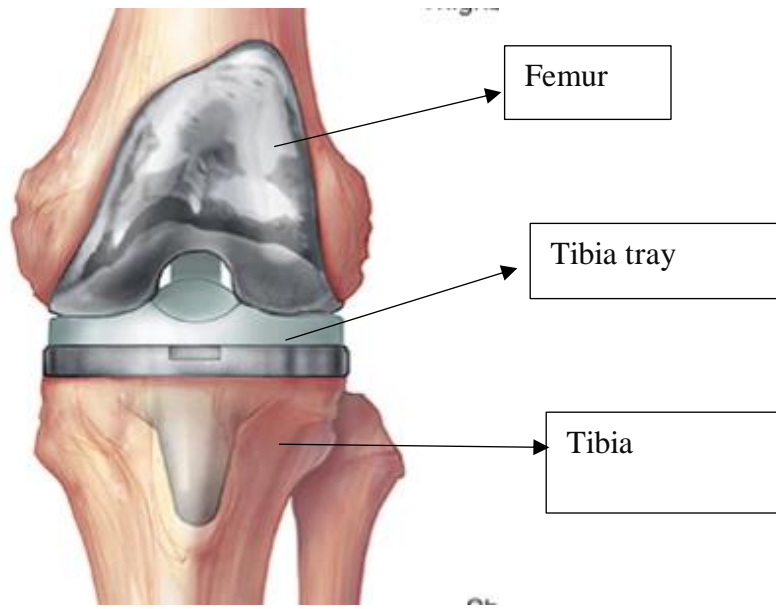


Figure 1-1: Total knee replacement surgery with femoral and tibia tray(<https://www.mayoclinic.org>).

1.2. Reasons for Total Knee Replacement Surgery

There are enormous reasons for a patient to require total knee replacement. Amongst the many reasons, arthritis is the most common [1,2]. The three most common types of arthritis which destroy the knee joint and surrounding bone includes osteoarthritis, rheumatoid arthritis, and post-traumatic arthritis [3,4]. Arthritis is an extremely painful disease of the knee, causing the patient to suffer high level of pain affecting normal everyday movement. Because of this loss of movement, an individual suffering from arthritis within the knee is confined to uncomfortable and sedentary living [3,4,5]. This type of living is non ideal, painful, as well as unhealthy. Inactivity, especially among older adults, greatly affects health and life expectancy. Damage due to arthritis such as aforementioned may lead to deterioration of the surrounding bone. This high level of pain affects mechanical strength leading to

decreased activity. The decrease activity further leads to deterioration eventually resulting in loss in bone density around the damage area.

When medication and other forms of treatment no longer become a viable option, a total knee replacement becomes the best option. Total knee replacement surgery restores the patient's ability to perform everyday activities without severe pain. In addition, severe arthritis can cause knee deformities, such as bowing in or out of the knee. A total knee replacement can restore the "natural" look of the knee if this type of damage is apparent. As previously outlined, follow up surgery is uncommon for total knee replacement surgery, indicating that this type of surgery is a viable and effective option for those suffering from immobility due to arthritis. Other reasons for the need of a total knee replacement surgery include but not limited to accidents and sports injuries.

1.3. Total Knee replacement Material

1.3.1. Stem

The stem is the portion of the replacement that fits into the bone. Titanium alloys have several amazing properties that make it a good fit for use as stem in medicine. Titanium, in its pure form, has a low density, high strength and a high level of corrosion resistance [5]. In addition, it is also non-toxic and non-magnetic - two properties that are specifically beneficial for use in biomedical applications [6,7]. Titanium alloys exhibit attractive properties such as biocompatibility, safety and ductility. Titanium (Ti) is used as an orthopedic and orthodontic implant material for excellent biocompatibility [7]. The process of dissolution of Titanium into body is very fundamental because titanium surface reacts spontaneously to form a stable and unreactive coating of titanium dioxide (Ti₂O), this coating prevents titanium element from the

reaction with body fluids [8]. Titanium is very biocompatibility, show high corrosion resistance, very low level of ion-formation capability, extremely low electronic conductivity due to the formation of the oxide inert layer. However, for this study since it is an in vitro study with a saw bone, aluminum was the test material that was used because of limitation in finance and because it is basically a testing process for the effect of Laser microgroove on an artificial tibia tray.

Cobalt-chromium alloys are also used in implants. They are considered highly biocompatible as well as titanium and have shown excellent short-term results in the United States and may be useful when utilized in specific patients [1]. Ceramic when coupled with ceramic balls is very strong material and provides low wear rate in an implant. Polyethylene is most often used as a liner in implant [6].

1.3.2. Bone cement

Bone cement is used in various orthopedic surgeries for both human and animals. Among the many materials with high potential for used as bone cement, polymethylmethacrylate (PMMA) bone cement has been used successfully many surgeries mostly because of its strong mechanical bonding with implant. PMMA bone cements commercially available as material with two components; liquid (MMA monomer) and powder (PMMA beads). These components are mixed in the ratio 2:1 to allow for the mixture polymerize. The current most commercially available human PMMA bone cements are Cobalt (Biomet, Inc.), Simplex (Stryker, Inc.), and Palacos (Heraeus Company). The current most commercially available animal PMMA bone cements are BioMedtrix, Patterson, Jorgensen Labs veterinary bone cement that was used in this study is shown in figure 1-2 below.



Figure 1-2: PMMA bone cement used in the study; Biomedrix 3 Veterinarian bone cement

Several drawbacks associated with PMMA bone cement limit its efficacy. Some of the drawbacks associated with PMMA include; inadequate adherence to the bone surfaces (no bioactivity) [11], it has a high exothermic reaction temperature [12] and it exhibits monomer toxicity [12]. Particularly, enough bonding strength of cement with the implant and bone is required for the design of optimal bone cement, which may be greatly influenced by the high exothermic temperature. It is important to determine temperature changes in the PMMA bone cements during curing and how the different level of curing time and temperature influences the mechanical properties of bone cement and bonding strength between implant and cement. The change of mechanical properties of bone cements with different curing time is required for their use in bone cement

1.4. Problem Statement

An ideal implant for TKR surgeries should ensure lifelong mechanical stability with the joining tissues [13]. Most often, the implant surface is inadequate, micromotions that

occur at the implant surface activate osteoclasts, which resorb bone around the implant and contribute to implant loosening and eventual implant failure [14,15,16]. A method to improve mechanical fixation of a TKR implant is clinically important and is the purpose of the proposed research project

1.5. Hypothesis

No study has reported the effect of LIM on a TKR implant surface on the mechanical performances in cemented TKR surgery. Is laser induce microgroove the solution to improve the mechanical strength of total knee replacement surgery? This is the solution being investigated in this study.

1.6. Motivation and Goals

The majority of cemented knee replacements fail due to implant loosening. One of the important factors that may affect implant loosening is the mechanical behavior of cement at the implant-cement interface. The motivation of this study is to design implant loosening free tibia tray for a dog to determine the efficiency so as to extend to human for orthopedic surgeries. The goal of the study is to understand how mechanical behavior of implant-cement interface is influenced by the change of mechanical design.

Laser-induced microgrooves (LIM) on a titanium TKR implant can increase the mechanical fixation of implant due to high contact surface area and transfer of force from implant to adjoining tissue [21,22,23]. No study has reported the effect of LIM on a TKR implant surface on the mechanical performances in cemented TKR surgery. This research has three main objectives.

1.7. Objectives

This study has three main objectives geared towards investigating the effect of laser induced microgroove on tibia tray. The objectives are;

Objective 1: To design a tibia tray for a dog by using a 3-D scanner and exporting the image into solid works. The samples were characterized by measuring the roughness

Objective 2: To design the experimental setup for use in Test Resource machine to measure the effects of grooves on the fatigue life of tibia tray implant of a canine total knee replacement systems.

Objective 3: To develop finite element analysis model of tibia tray implant of a canine total knee replacement and determine the effect of groove on stress distribution around the implant.

1.8. Organization of the thesis

The outline of this thesis was organized into five chapters; chapter 1 is the introductory chapter while from chapter 2 to chapter 5 is organized to such as to attain the above three main objectives of this project.

Chapter 1

The first chapter of this thesis gives a brief introduction, 3-D scanning and exporting the image into solid works. Solid works was used to design the tibia and CNC machine was used to machine the part. Six samples were made, and laser machine was used to produce laser microgrooves on three of the samples. The samples were characterized by measuring the roughness.

Chapter 2

This chapter focuses on design the experimental setup for use in Test Resource machine to measure the effects of grooves on the fatigue life

Chapter 3

The third chapter of this research focuses on performing finite element analysis on the groove and the non-groove tibia tray and compare the results with the test result.

Chapter 4

The last section of this study gives the Conclusion and future work

Chapter 2 Tibia Tray Design Using Solid Works, Manufacture Using CNC Machine and Characterization Using a Profiler.

2.1. Abstract

Different knee implant models have been studied in several different articles [27-29]. In the last decades major developments in knee implant designs have improved the outcome of the surgery in a way that the lives of those with implants have greatly improved and has also increased the value of life to people with arthritis, people with injured knees and war veterans. Artificial joints should satisfy certain design requirements, i.e., they should be ergonomical and biocompatible.

This study designs tibia tray using solid works, manufacture using CNC machine and characterize the surface of the manufactured tibia tray using 3-D optical profiler. The need for an implant has been established and the use of titanium and cement for an in vitro study has also been established. This study used an artificial saw bone of a dog and aluminum to design the tibia tray used for this study. Artificial bone was used since this is an ex vivo study and real bone is not possible to acquire. Aluminum was use because it is relatively cheap and available and show some similar characteristics to aluminum in an implant.

2.2. Introduction

Different studies have design tibia tray using different materials and shapes in an endeavor to mimic the natural knee. The important issue is the biomedical product design and development. Other theories and experiments have studied and contributed to the process of strengthening and optimizing the design and production of tibia tray in an attempt

to improve the implant performance through the examination of the wear and tear of design with time [25, 30].

Other studies have studied the coverage comparing anatomic and symmetric tibia tray coverage. In recent study, the anatomic tray when compared to symmetric trays and asymmetric trays have proven to show significantly, a higher surface coverage [39].

2.3. Summary

This study designed tibia tray using solid works, manufactured using CNC machine and characterized the surface of the manufactured tibia tray using 3-D optical profiler. Artificial bone was used since this is an ex vivo study and real bone was not possible to acquire. Aluminum was use because it is relatively cheap and available and show some similar characteristics to aluminum in an implant.

The objective of this study was to design a tibia tray for a dog by using a 3-D scanner and exporting the image into solid works. Solid works was used to design the tibia and CNC machine was used to machine the part. Six samples were made, and laser machine was used to produce laser microgrooves on three of the samples. The samples were characterized by measuring the roughness.

2.4. Materials and Methods

2.4.1. Protocol to Fabricate Tibia Tray Implant

This includes using MeshLab for pre-processing of an obtained CT scanned tibia model, SolidWorks design of each model under examination, as well as FE simulation modeling techniques.

The following steps were performed to create each studied assembly, for each geometry type and size. This process was kept consistent in order to ensure results obtained from each assembly had minimal variability in model formation.

(a) 3-dimensional scan model of a dog tibia-fibula was obtained as a .dxf format (Drawing Exchange Format).

(b) The model was Imported into MeshLab for model simplification, exported as an .IGES file type (Initial Graphics Exchange Specification). Then the file was further imported into SolidWorks.

(c) Tibia tray was designed on the scanned model to ensure efficiency and dimensional specifications. This was done so as to also ensure model assembly without so much offsets

(d) Experimental setup was designed using solid works to mimic the femoral bone so to perform fatigue test on the assembly.

2.4.2. 3-D Scanning

The bone was scanned using an Open-frame desktop 3D scanner. This scanner-type was use because it's flexibility in terms of 3D scanning area but they should be used in a compartment with a constant source of light and the light must not be too bright. This desktop 3D scanners is made up of a light projector or cameras that is mounted on a tripod to ensure stability and more accurately scanned image, figure 2-1



Figure 2-1: Open-frame desktop 3D scanners

After performing several scanning procedures, the most accurate 3-D scan that was obtained is shown in the figure below;

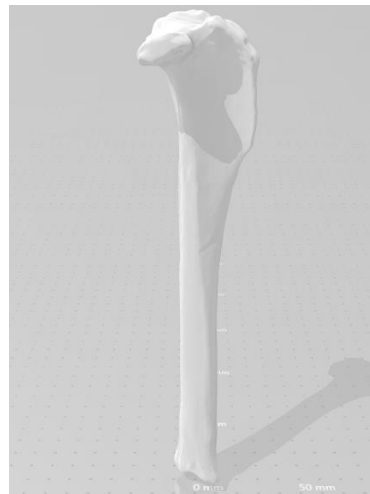


Figure 2-2: Scanned image of a Dog Tibia

2.4.3. 3D Modeling

In order to ensure accuracy of the tibia tray for this study, the scanned tibia-fibula was imported into MeshLab for model simplification, exported as an .IGES file type (Initial Graphics Exchange Specification), then imported .IGES file into SolidWorks, then repair

geometry. Using the scanned data as reference, the tibia tray was designed on the scanned bone to get the design with groove and the design without grooves as shown in figure 2-3.

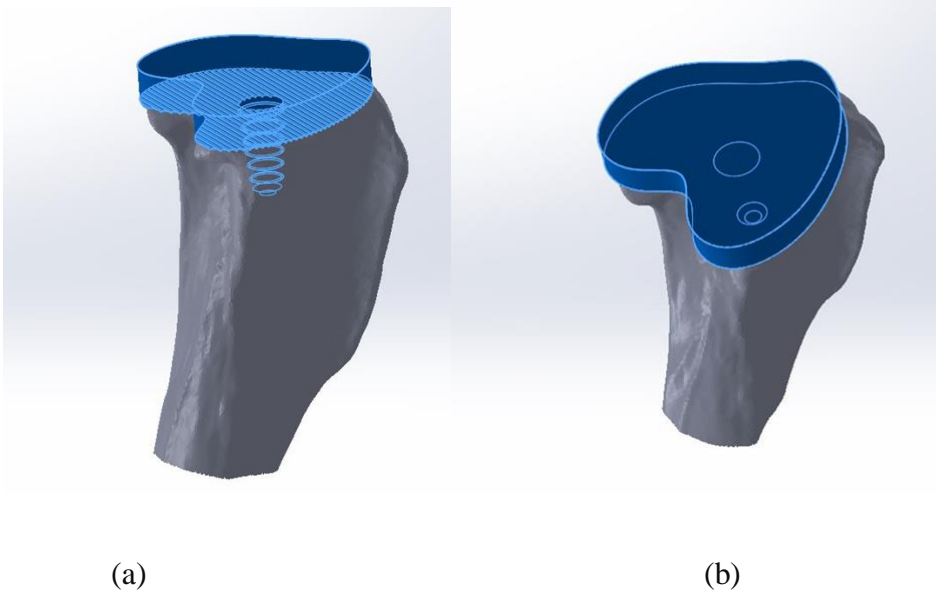


Figure 2-3: Design of a tibia tray on scan tibia-fibula. (a) Model with microgrooves. (b) Model with no grooves.

After the designing the tibia tray, the scanned bone was suppressed to get a perfect design of the tibia tray. Six sample were machined using CNC machine. Laser microgrooves were performed on three of the samples as shown in the image in figure 2-4 below;

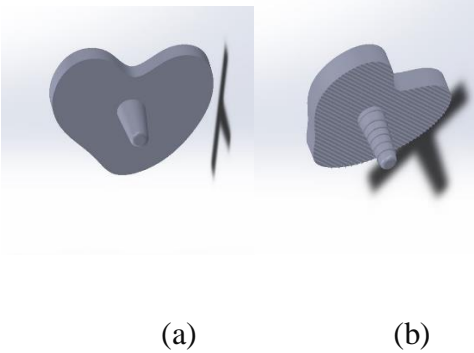


Figure 2-4: Image of the tibia tray ready for machining. (a) Smooth tibia tray. (b) Tibia tray with Microgrooves.

The radiuses of solid works file shown above in figure 4 was clearly defined for machining using a CNC machine. The data is shown below;

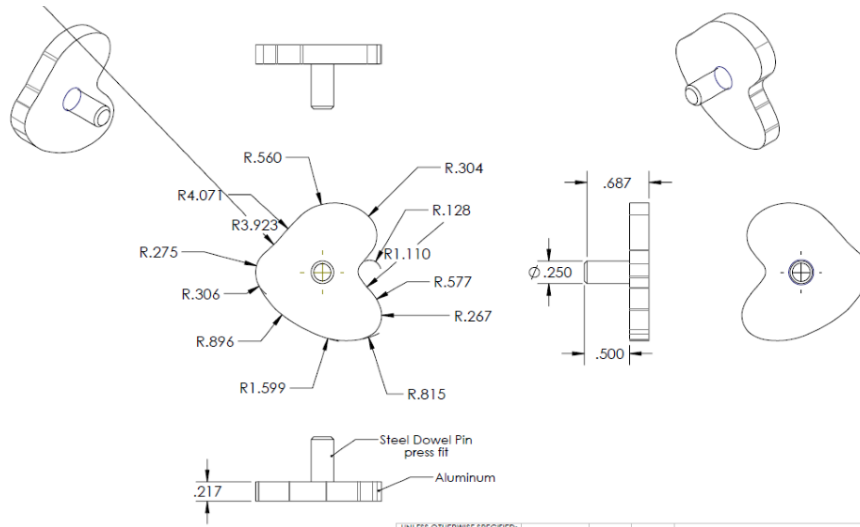


Figure 2-5: Machine data

2.5. Results

Six samples were machined using CNC machine and the samples were characterized using a profiler to determine the roughness. Figure 2-6 smooth sample (sample with no grooves) after it has been produced using CNC machine. These samples have a heart shape. This shape is the most appropriate shape that will cover more surface area and will be symmetric together with the bone sample. This smooth sample showed an average roughness of 6 microns as showed in figure 8. This roughness is further indicated in detail in figure 2-8. This roughness is important in cement adhesion and is of greater importance when dealing uncemented implant to improve bonding between the bone and the implant.

The rough sample (sample with grooves) was design in solid works and manufactured in CNC machine as well and was engraved with microgrooves using laser machine for 6hrs

[figure 2-9]. The samples with microgrooves were characterized in profiler. The sample with groove had a mean roughness of 11.41 micron [Figure 2-10 and Figure 2-11].

Figure 2-6 is the result of the design after being machined using CNC machine. The samples were well polished. Figure 2-7 shows the variation in roughness of the smooth tibia tray. It gives the roughness map indicating areas of maximum roughness and minimum roughness.

The average roughness of the sample is indicated in Figure 2-8. This figure indicates the minimum roughness, the maximum roughness, the average roughness and the mean height of roughness.

Figure 2-9 is the result of the tibia tray after it has been engraved by the use of a laser for 6 hours. This figure gives the visibility of the grooves of the tibia tray. Figure 2-10 shows the roughness map of the tibia tray with grooves. Figure 2-11 gives the minimum height of roughness, maximum height and average height.



Figure 2-6: Tibia Tray Machined Using CNC Machine

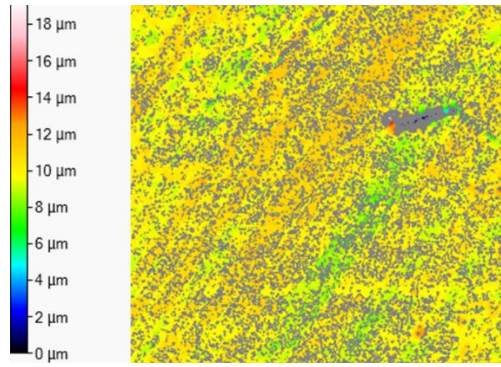


Figure 2-7: Profiler Image of Smooth Sample Roughness.

Area Roughness

General			
Average	9.891	µm	Mean height
Minimum	0	µm	Minimum height
Maximum	19.23	µm	Maximum height
Range	19.23	µm	Maximum - Minimum

Figure 2-8: Details of Roughness of Smooth Tibia Tray



Figure 2-9: Tibia Tray with Micro Grooves

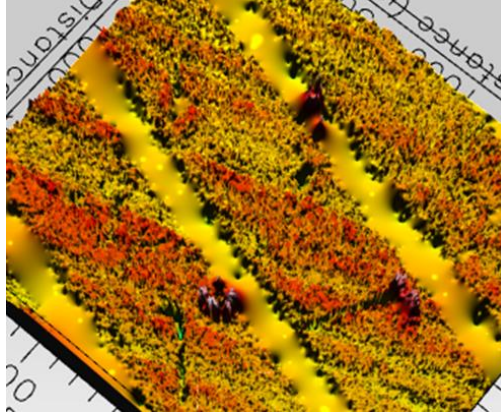


Figure 2-10: Profiler Image of Tibia with Grooves

Area Roughness

General			
Average	11.41	μm	Mean height
Minimum	0	μm	Minimum height
Maximum	18.25	μm	Maximum height
Range	18.25	μm	Maximum - Minimum

Figure 2-11: Details of Mean Roughness of Tibia Tray with Grooves

2.6. Conclusion

To convert the saw bone into a form readable by the computer, 3D scanner was used to get the exact dimension, solid works was used to design the implant. The measurement was made effective on the scanned components and proper identification of the different shapes of the bone was made appropriate.

This study successfully designed, manufactured and characterized 6 tibia tray samples for an in vitro study using canine bone. Upon the six samples, three were smooth and three

were engraved with laser microgroove. These sample showed every good characteristic ready for mechanical test (static and cyclic fatigue test) in vitro.

The samples with no grooves show an average roughness of 9 microns while the sample with grooves shows an average roughness of 19 microns. These values are very important in that it presents the surface characteristics of the sample.

Chapter 3 Experimental study to evaluate the effect of groove on static and cyclic load.

3.1. Abstract

When a total knee implant is designed and manufactured, several tests are performed on the sample to ensure lifelong mechanical, biomedical and biocompatibility stability. This study designs the experimental setup for use in Test Resource machine to measure the effects of grooves on the fatigue life. The test setup is designed to perform static and cyclic fatigue test. Physical measurement of the cross-section of the tibia tray was measured to determine the exact dimensions of the experimental setup. These measurements were done to design a perfect setup to mimic the human femoral tray that will help perform the fatigue test.

This study designs and assemble experimental setup using solid works and CNC machine. The sample is then machined using CNC machine. After all the parts are produced, they are assembled and mounted onto Test Resources for the experiment. Two sets of tests are performed using the test run; the cyclic fatigue test and the static compression test. These two tests were performed to establish the effects of laser induced microgrooves on cemented tibia tray implant. The first sets of tests were performed, and the sample was allowed to relax before the last sets of tests were performed until the sample failed. These tests were performed until failure was established and each sample was analyzed using x-ray images to visualize any internal change in structure. The samples with grooves showed greater stability because it needed a greater force to fail after being subjected to the same conditions with the samples with no grooves.

3.2. Introduction

An ideal implant should ensure lifelong mechanical, biomedical and biocompatibility stability. Most implant suffer from micromotions that occur at the implant surface. This micromotions activate osteoclasts, which resorb bone around the implant and contribute to implant loosening and eventual implant failure. After an implant is designed, to ensure that all the properties are maintained, the implant is subjected into test to measure the mechanical strength and durability.

Another test that is performed on tibia tray is the compression test to determine the point of failure to establish the maximum yield strength. Other test that are performed in different clinical study are Component Pull Tests and Component Ultimate Strength Tests [38].

3.3. Materials and Method

3.3.1. Material

This experiment was carried out in vitro using a sawbone. The rationale behind this experiment is based on the fact that Since the amount of implant-to-bone contact area determines the mechanical stability of implants [24,13], the effect of the fabricated laser induced microgrooving (LIM) topography on a custom-made tibial tray implant will be measured by means of in vitro mechanical examinations using an artificial dog tibia model.

3.3.2. Experimental Setup

Four different models were designed and machined using solid works and CNC machine respectively. Figure 3-1 shows part a of the experimental design.

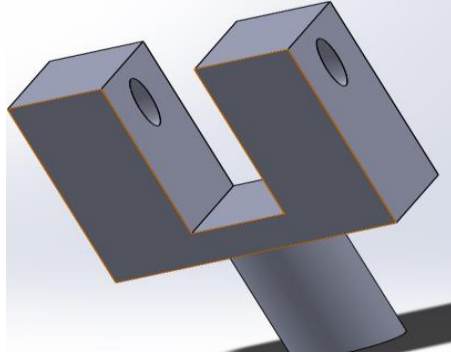


Figure 3-1: Part (a) with a Point Attachment to the Compression Machine

The second experimental part was part (b) that could perfectly fit into part (a) as shown in the image below;

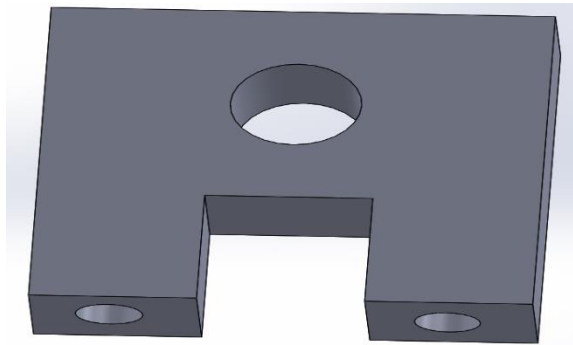


Figure 3-2: Experimental Part (b)

The third part, part (c) was the part that will hold the bottom of the bone as shown in the Figure below;

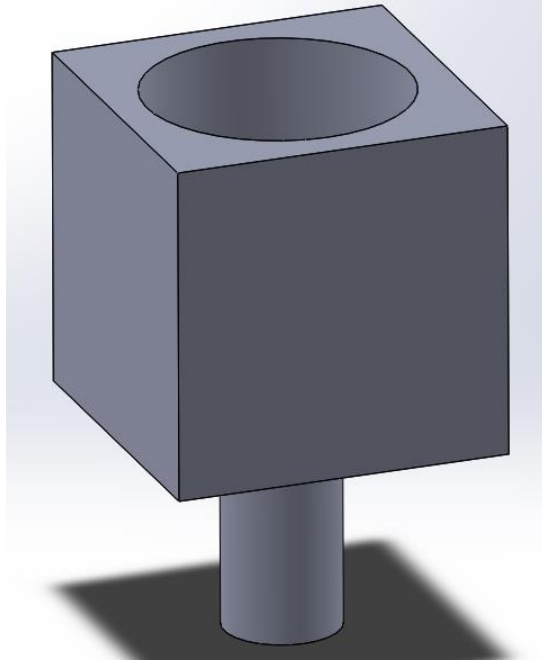


Figure 3-3: Bottom Part, Part (c).

Part a, b, and c were produced using the CNC machine. The experimental setup was then assembled in solid works as shown in Figure 3-4 below;



Figure 3-4: Experimental Setup Design

The samples were manufactured using CNC machine as shown in Figure 3-5 below.

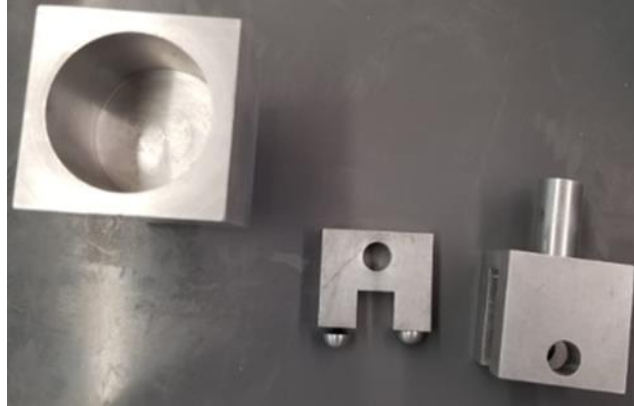


Figure 3-5: Test Tools Designed and ready for Assembly onto Test Resources for Experiment.

3.3.3. Sample preparation

A) Bone Preparation

Six dog sawbones were cut following strict surgical procedure as shown in figure 3-5 and figure 3-6 below;



Figure 3-6: The Process of Cutting the Sawbone



Figure 3-7: Six Saw Bones cut according to Surgical Procedure

A 0.25in diameter hole was drilled into the bones using a drill bit to a depth of 0.5in to effectively accommodate the tibia tray as shown in figure 3-7.



Figure 3-8: Tibia Fibula Bone with a Hole to Accommodate Tibia Tray.

B) Cement Preparation

2.4g of cement (figure 3-8) was used with 600 micro liter of liquid. The mixture was stirred up for a few minutes to obtain a homogenous mixture.



Figure 3-9: Preparation of 2.40g of PMM Cement

B) Fixation Technique

The big challenges in orthopedic and orthodontic are the failure of the implant at the implant-cement interface [20,26]. Cemented fixation is more common for osteoporotic bone, where the bone cement is used to attach the implant to the bone. However, cement less fixation is available and is more expensive. But this study focuses on cemented in vitro analysis of a dog bone.

To ensure the effectiveness of the implant, the tibia tray was press-fit at a load, $F = 70 \text{ N}$ during the period of bone cement polymerization to ensure resemblance of the surgeons' pressure on the implant and avoid wrong position of the implant [20, 26]. This force will reconcile an average stress of 60 kpa [20].

From the design, the total surface area of the designed tibia tray is $1.28 \cdot 10^{-3} \text{ M}^2$ and the average mass of a dog is 30kg. dividing the mass by 4 to get the average weight on each leg gives an approximate average mass of 7.5kg per leg of the dog.

The cement was prepared and press-fit with a mass of 7kg for 30 minutes as shown in the figure 3-9 below;



Figure 3-10: Fixation of Implant into The Bone

3.3.4. Fatigue and Compression Test

A scientific method used for the determination of the behavior of materials under fluctuating loads. A specific mean load and an alternating load were applied to the samples with grooves and samples without grooves and the number of cycles required to produce failure (fatigue life) was recorded. Loads were applied axially, in compression. Data from fatigue testing were presented in an S-N diagram which is a plot of the number of cycles required to cause failure in a specimen against the amplitude of the cyclical stress developed.

A compression test is a scientific method used to determine the behavior of materials under a compressive load. Compression tests were conducted by loading the test samples in

test resources, and then applying a force to the samples by pressing both ends of the samples together.

After performing the test, the sample is analyzed by plotting deformation versus the applied load recorded. The compression test was used to determine elastic limit, proportional limit, yield point, yield strength, and compressive strength [33].

3.4. Design of Experiment

A) Fatigue Test

Four samples were prepared and mounted on test resources as shown in figure 3-10 and figure 3-11 below for the fatigue test analysis.



Figure 3-3-11: Mounting of the Sample on Compression Test Machine



Figure 3-12: Complete Setup of the System for Fatigue Test

In order to mimic a real time scenario and to ensure the validity of the experiment, the mean average load was set at 150N (which is the maximum load a dog knee can withstand), the amplitude set at 30, the frequency set at 1Hz and the experiment was for 100000 cycles and observed under high speed camera. The X-ray of all the samples were taken before and after every 100000 cycles to record every change. The details of every experiment can be shown in figure 3-12 below. Fatigue test was performed on two groups of sample; the samples with grooves and the samples with no grooves.

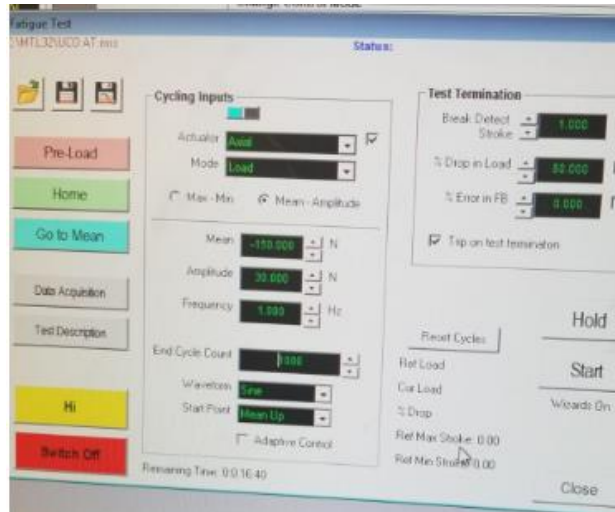


Figure 3-13: Details of Fatigue Test

3.4.1. Compression Test

Two samples were used for compression test.

1) Sample Without Grooves

Compression test was performed on the sample without grooves by increasing the displacement at a rate of 0.05mm and the system automatically recorded the force until failure. The automatically stops when it records a failure, that is at the point where the displacement is increasing but the force is reducing.

2) Sample with Grooves

Compression was also applied on the sample with grooves using test resources by increasing the displacement at a rate of 0.05 mm and measuring the axial force in Newtons at every instant. This process was set to run automatically in test resources and the force being recorded until at the point of failure, where an increase in displacement is not accompanied by a corresponding increase in force. This is point of failure where the implant has failed.

3.5. Results

3.5.1. Fatigue Test

A) Sample Without Grooves

After running the experiment for an axial load of 150N, amplitude of 30, frequency of 1Hz, and 100000 cycles, the data from the first experiment shows that as time went on, the amplitude of oscillation was slightly increasing until it arrived at a constant as shown in the graph below in figure 3-14;

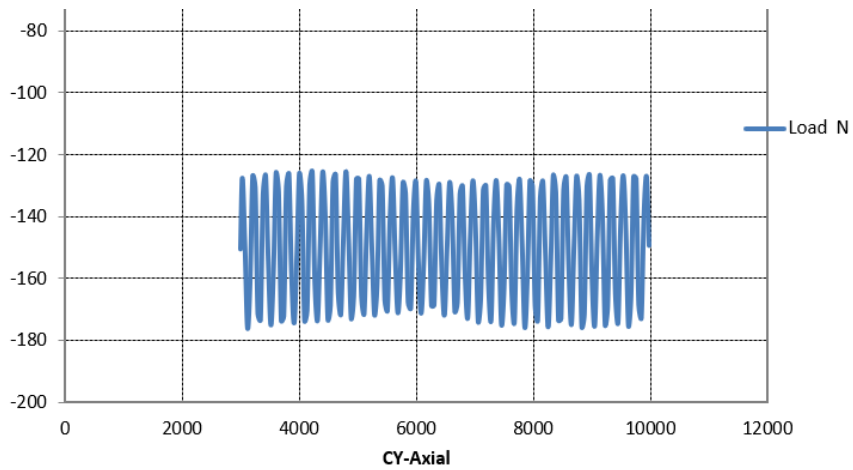


Figure 3-14: Changes in the Amplitude of Oscillation as a Result of Fatigue Test.

X ray image of each sample with no grooves was taken before the experiment and after to help detect any cracks or changes in internal structure of the implant (Figure 3-15).

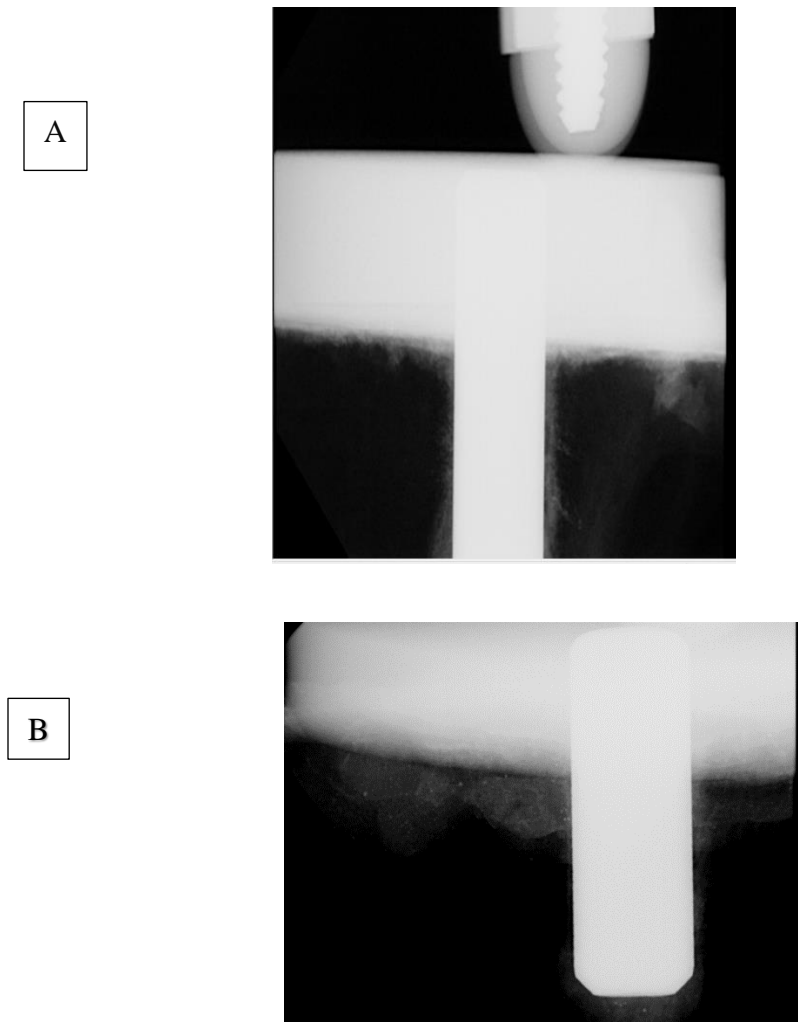


Figure 3-15: X-ray images before and after fatigue test. (a) before fatigue test (b) after fatigue

Figure 3-15 shows the x-ray of the sample before and after the fatigue test and there are some small changes. These changes indicate the effects of the fatigue test.

B) Tibia Tray with Grooves

Tibia tray with grooves was set to run with the same condition as with the non grooves. The test run was set up with axial load of 150N, amplitude of 30, frequency of 1Hz, and 100000 cycles, X-ray image of the sample with groove was taken. The most visible of all the images is shown in figure 3-15 below;

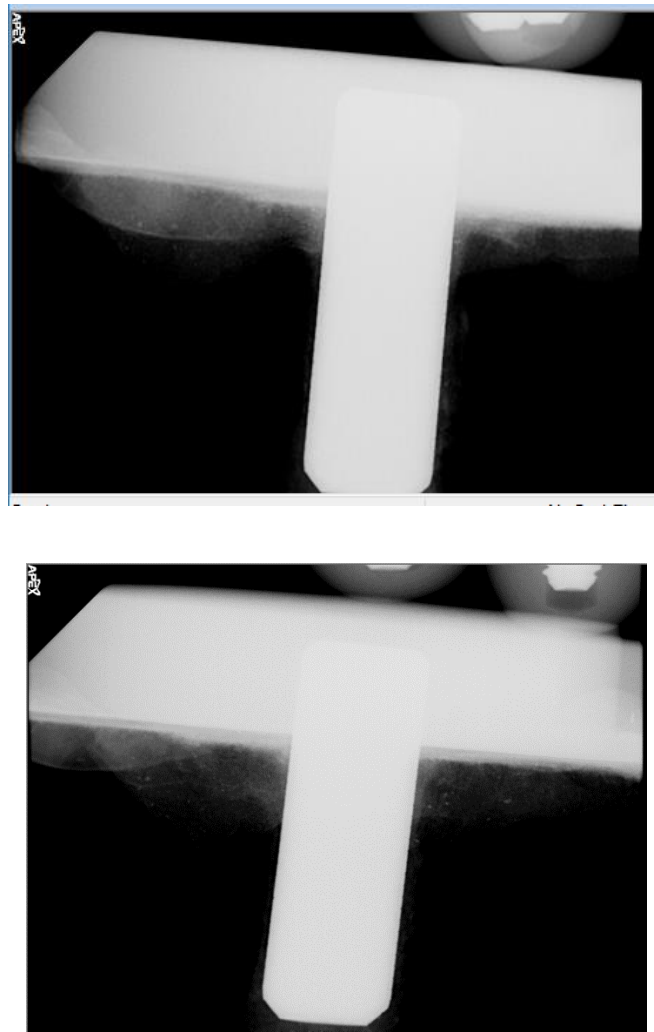


Figure 3-16: X-ray images grooved sample before and after fatigue test. (a) before fatigue test (b) after fatigue test

Figure 3-16 show the changes that occurred in the internal structure. In the image, there are some traces of compression in the tibia-cement interface. This result shows the effect of fatigue test and other changes in the internal structure of the implant.

3.5.2. Compression Test

A) Sample Without Grooves

It was observed that the sample without grooves showed the force was increasing at a constant rate before failure. The sample without groove failed at a force of 550N. Figure 3-17 shows the increase in load and stroke until failure at a load of 550. Figure 3-18 shows deformation characteristics of the sample after failure and the changes that occurred at the cement-implant interface.

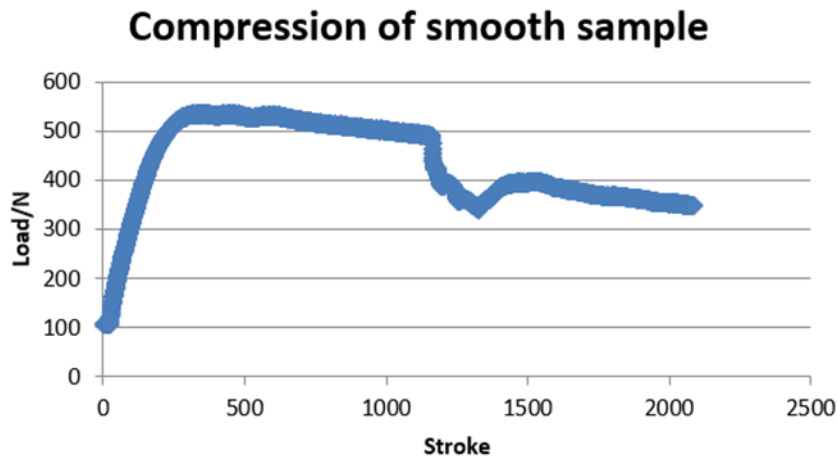


Figure 3-17: A Graph of Load Vs Stroke to Indicate the Point of Failure for Tibia Tray Without Grooves

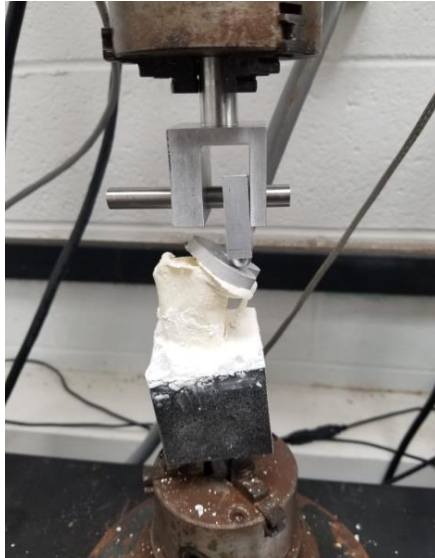


Figure 3-18: Failure Characteristics after the Sample Failed

B) Sample with Grooves

It was observed that the sample with grooves showed the force was increasing at a constant rate before failure. The sample with groove failed at a force of 640N. Figure 3-18 shows the increase in load and stroke until failure at a load of 640N.

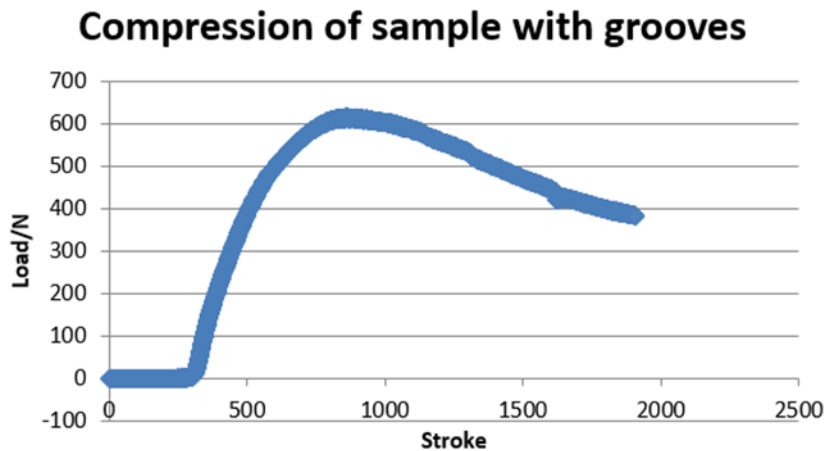


Figure 3-19: A Graph of Load Vs Stroke to Show the Changes in Tibia Tray with Grooves

3.6. Conclusion

The experiment setup was design, machined and assembled (figure 3-12) after which they were mounted onto test resources. Fatigue tests were performed.

After performing four fatigue experiments, it was observed that all the samples were generally showing the same trend. There were some traces of cracks and the axial distance was increasing up to a about 0.017mm then after about 10000 cycles, the system was stabilized. Some traces of cracks were observed but could not be analyzed properly with currently available equipment. The samples with grooves showed some significant stability when compared with the samples with no grooves. This result led to the final experiment to completely compress the sample using a static load to failure.

For the compression test, it was observed that the samples with grooves showed more stability as the force was increasing at a constant rate before failure. However, the sample with grooves failed at a force of 640N while the sample with no grooves failed at a force of 550N. (figure 3-17 and figure 3-19). The deformation characteristic shown in figure 3-18 indicates the change that occurred at the cement-implant interface.

Chapter 4 Finite element analysis to evaluate the stress distribution around tibia tray implant due to static and cyclic load

4.1. Abstract

This study, started from the designing 3D model of the dog tibia tray using a dog knee prosthesis, 3D model of tibia tray was designed and bonded with a dog bone. The study investigates the effects of laser induced microgrooves on cemented knee implant fixation using finite element analysis. Using AnsysWorkbench16.0 Engineering tool, the deformation and the strain and stress maps were obtained for cemented total knee replacement implant with grooves and for samples without grooves. Different loading force were considered ranging from 100N to 600N. In the study, each tibia tray assembly considered two cases; samples with grooves and samples with no grooves respectively. The results, confirmed by mechanical simulation, suggest that the samples with grooves had more stability than the samples without grooves.

4.2. Introduction

Finite Element Analysis (FEA) with ansys workbench is a technique that uses the finite element analysis method to analyze an engineering design and determine effects of applied stresses on the design [39]. FEA also help determine all points of potential weakness in an Engineering design before it is properly manufactured [38]. This analysis was carried out by using a fine mesh and point of contact between the bone-cement -implant interface. Finite element (FE) modeling allows implants to be tested and has been used in several biomechanical studies [27-31].

FE method is used to evaluate biomechanical characteristics of cancellous bone on patellofemoral surgical replacement of a joint [31,32,33]. The influence of different designs of the joint area on tibial component fixation, kinematics and clinical outcome after a cemented total knee arthroplasty was studied in [33]. In knee implant study [27, 33,40], the finite element analysis method is used to simulate the loading conditions applied to the prosthesis device during the walking cycle. The objective was to perform finite element analysis on the groove and the non-groove tibia tray and compare the results with the test result.

4.3. Method

4.3.1. Geometry

The scanned and designed model was stored in .xt format. The model was imported into ansys workbench. This process was done to ensure accuracy and allow for the model to be formed as an assembly of all imported models for each TKR stem type under study. Doing so allowed for consistency in the assembly build, in order to avoid any differentials from assembly to assembly. The same procedure was done for the sample with grooves and the sample with no grooves. The properties of the assembled design used in this study is shown in table 4-1.

Properties	Unit	Bone	Aluminum	PMM cement
Density	Kg/m ³	1550	2770	1190
Young's modulus	Mpa	1*10 ⁵	7.1*10 ⁴	3.3
Poison ration		0.45	0.33	0.39
Shear modulus	Mpa		2.6*10 ⁴	1.1871*10 ⁵
Compressive ultimate strength	Mpa	60	310	120
Compressive yield strength	Mpa	60	280	120
Tensile ultimate strength	Mpa	70	310	69
Tensile yield strength	Mpa	70	280	70

Table 4-1: Properties of Bone and Aluminum used Simulation

4.3.2. Mesh

The imported model was meshed as showed in figure 31. The fine meshing was applied.

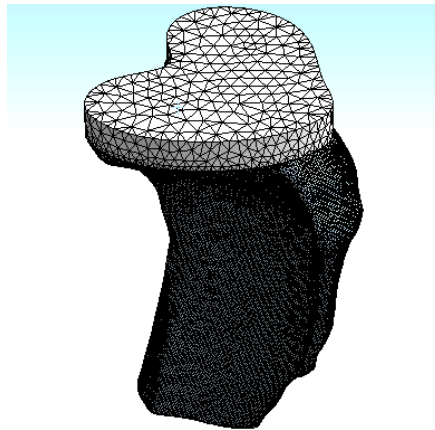


Figure 4-1: Fine Meshing

4.3.3. Boundary Conditions

Bonded contact was defined for the tibia tray and bone sample. Bonded contact was defined to account for the cement in this in vitro analysis.

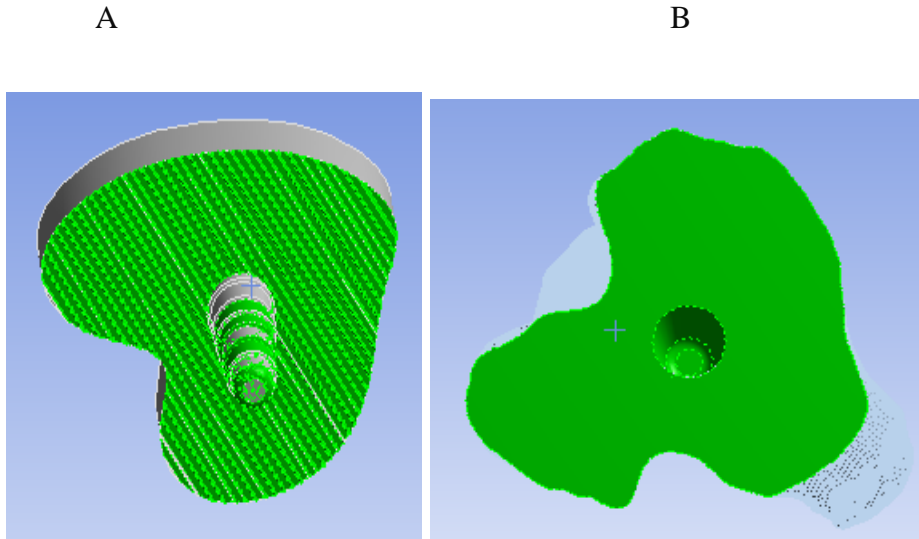


Figure 4-2: Bonded Contacts Between Bone and Tibia Tray

4.3.4. Post Process Output

A) Deformation

The deformation of the samples with groove and the sample with no groove were analyzed using ansys workbench. The deformation characteristic showed greater deformation at one side of the sample where the bone had little surface area. Figure 4-3 and 4-4 shows the distribution of deformation.

B) Stress field

The stress field of the sample with groove and the sample with no groove was also analyzed using ansys workbench and the stress field showed high stress only at the point of contact.

4.4. Results and Discussion

4.4.1. Samples without Grooves

The fatigue test simulation results for the sample with no groove showed that only a fraction of the force was transferred from the tibia tray into the bone as shown in the figure 4-3 and figure 4-4. The deformation was exported and plotted to show the variation in deformation with load as shown in figure 4-8.

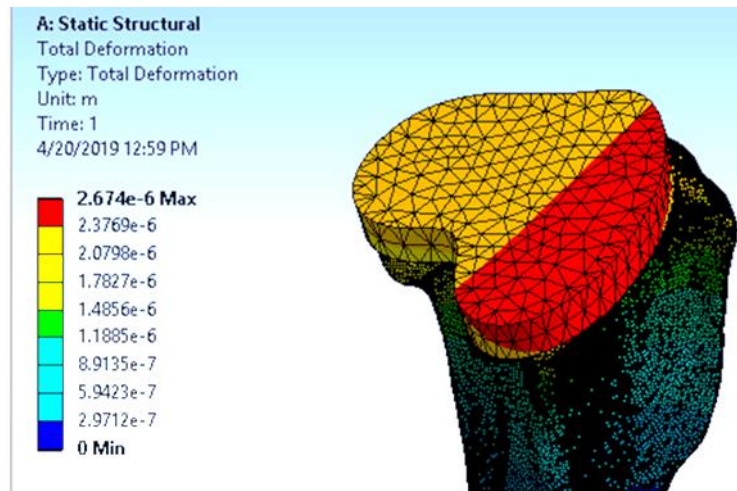


Figure 4-3: Deformation Characteristics of Top View of Cemented Tibia Tray on Bone

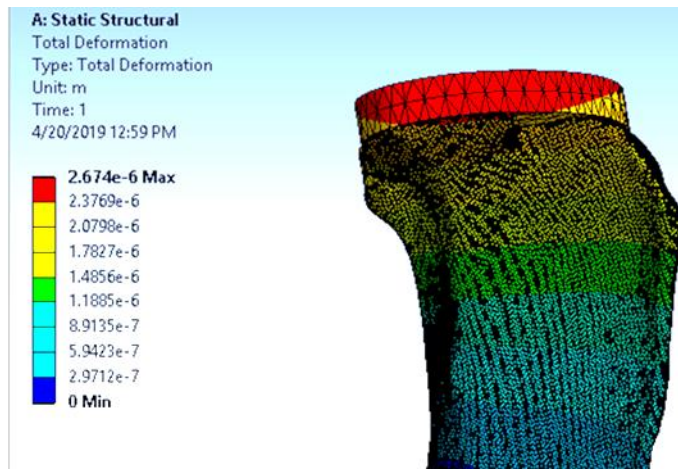


Figure 4-4: Side view of cemented tibia tray

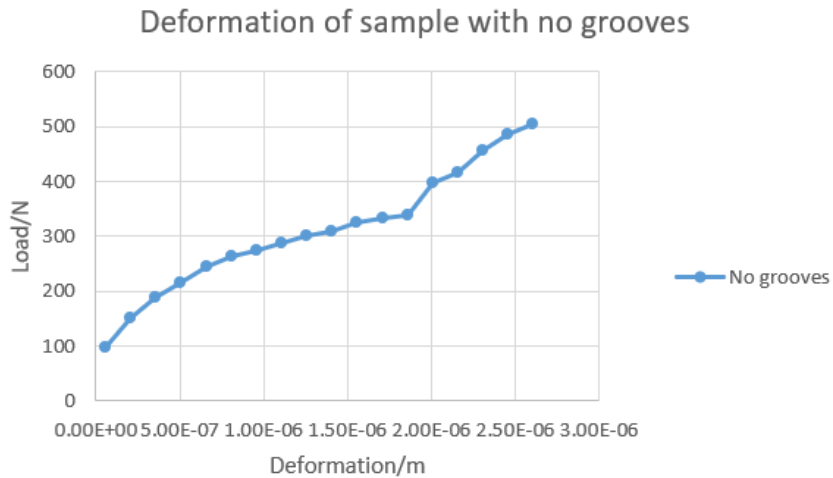


Figure 4-5: Variation of Load Against Deformation for Sample Without Groove

4.4.2. Samples with Grooves

The sample with grooves showed a field of deformation characteristics that was somewhat similar to that of the sample with no grooves but there was some difference in the deformation values. The samples with grooves showed some stability with increase in load accompanied by increase in deformation up to a force of 600N. A graph to show the deformation characteristic is shown in the figure 4-9 below:

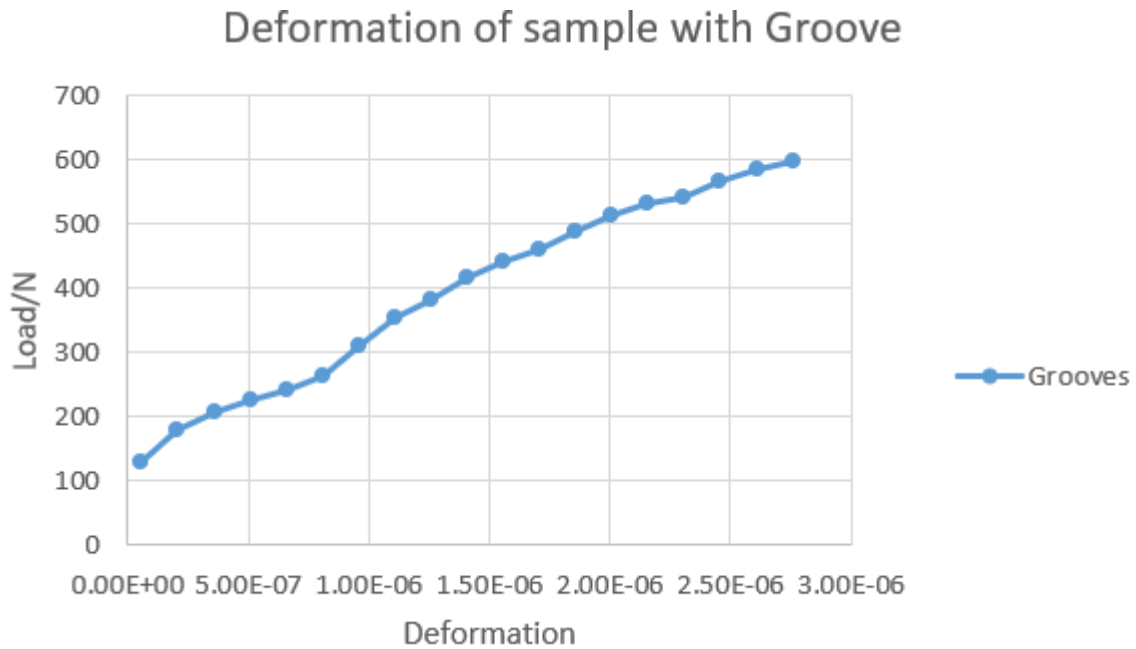


Figure 4-6: A Graph of Load Against Deformation for Sample with Groove

4.4.3. Comparison of result with experimental result

A) Samples with Grooves

The experimental result show that at a force 640N, the sample failed. The simulation showed that at a force of about 640N there was a deformation or displacement of 0.003mm at the interface.

This result show that the sample will groove will experience failure at a force of 640N.

B) Sample with no Groove

Experimental result for sample with groove showed a failure at 540N while the simulation showed a deformation of 0.025mm at a force of 540N.

The sample without grooves have less surface area for the cement to adhere and as such the sample with no groove will experience failure at a force of 540N.

4.5. Comparison of DIC Strain and FEA Strain

During the experiment, some data was collected and used to analyze the strain using the DIC method. The result of the strain from the DIC method is shown in the figure below.

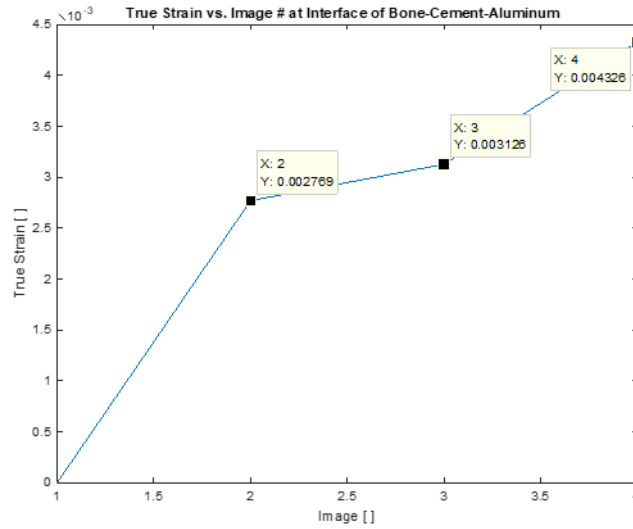


Figure 4-7: Strain obtain from DIC

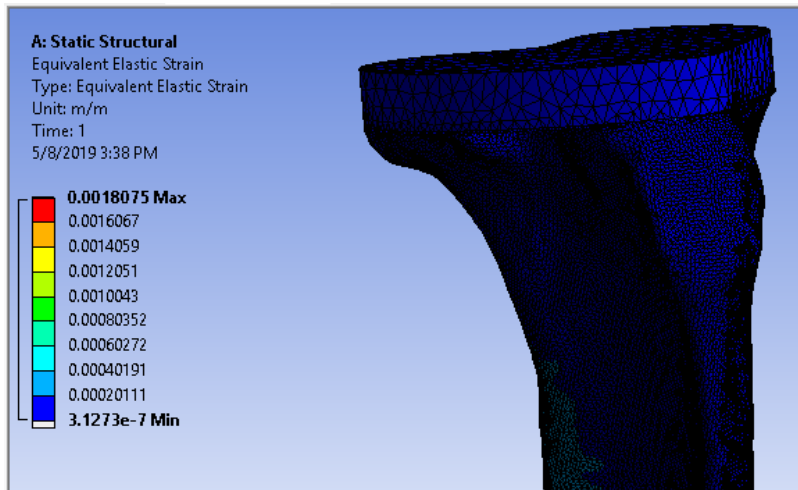


Figure 4-8: Equivalent Elastic Strain at 11000 cycles

No	Cycles	DIC	FEA	Error
1	1	0.002769	0.001808	34.72373
2	11000	0.003126	0.001808	42.16251
3	21000	0.004326	0.001808	58.2062

Table 4-2: The percentage Error for different Cycles in DIC and FEA

The percentage error shows a constant value for the FEA analysis for cycles while the strain value for DIC is increasing. This result may be due to different changes in the geometry of the sample from the scanned model.

4.6. Conclusion

In this study, starting from the design model of the tibia tray with grooves and dog tibia tray with no grooves and existent of knee prosthesis, often used in total knee arthroplasty, 3D model of tibia tray with grooves and tibia tray with no grooves were designed. The bone properties and the tibia tray properties were defined as well as the bonded contact to account for the use of cement in this study. Using AnsysWorkbench16.0 software, the stress and displacements maps are obtained for tibia tray with grooves and tibia tray with no grooves. The Finite Element Method is used to investigate the effects of tibia tray with grooves and tibia tray with no grooves and graphs are used to show the deformation at different loads. The findings of this study confirm that the samples with laser induce microgrooves have greater stability than the samples with no grooves. The main advantage of the numerical simulation is that they can be done in order to evaluate the biomechanical behavior of an animal joints without an invasive intervention. A finite element analysis of the normal and prosthetic knee model will help surgeons and biomechanical researchers to develop improved devices for rehabilitation movements of patients suffering diseases.

Chapter 5 Conclusion and future work

5.1. Conclusion

This study was conducted based on three objectives:

1. The very first objective of this study was to design a tibia tray for a dog by using a 3-D scanner and exporting the image into solid works. The samples were characterized by measuring the roughness
2. The second objective was to design the experimental setup for use in Test Resource machine to measure the effects of grooves on the fatigue life.
3. The third objective was to perform finite element analysis on the groove and the non-groove tibia tray and compare the results with the test result.

This study found the following as per objective;

1. The average height of roughness for smooth tibia tray was 11 micrometer while that for the tibia tray with groove was 100 micrometer. For the smooth tibia, the roughness did not affect the stability much but for the sample with grooves, the roughness was of utmost importance because it improved the stability of the sample.
2. The experiment was designed and performed. The conclusion from the experiment was that there was no great damage from the fatigue test in vitro. The samples showed a great stability and there was very little transfer of stress from the designed model to the bone. However, compression test revealed the stability of the sample with grooves. This also shows that for this study, the designed was very stable and working properly.
3. The simulation from ansys workbench showed very little trace of transfer stress from the designed sample into the bone. The stress was also distributed at one side of the circumference of the bone model. However, the maximum deformation was recorded from

the sample with no grooves. The smooth sample had a maximum deformation of 0.025mm while that from the sample with grooves was 0.03mm.

5.2. Future Work

This study was carried out in vitro and the cement was used to bond the tibia tray into the bone. The design of a tibia tray with laser microgrooves has proven to be a good model for future studies. For future work, it will be very imperative to perform this experiment in vivo with no cement and monitor the effect of laser induced microgrooves in relation to the bone cells in the surrounding.

References

1. "Knee Replacement Statistics Infographic." Knee Replacement Statistics. N.p., n.d. Web. 28 Oct. 2014.<<http://www.healthline.com/health/total-knee-replacement-surgery/statistics-infographic>>
2. "2012 AAOS Annual Meeting." 2012 AAOS Annual Meeting. American Academy of Orthopaedic Surgeons, 10 Feb. 2012. Web. 30 Jan. 2015.
3. HCUP FACTS AND FIGURES statistics on Hospital-Based Care in the United States, 2009. http://www.hcupus.ahrq.gov/reports/factsandfigures/2009/pdfs/FF_report_2009.pdf
4. Labek, G., M. Thaler, W. Janda, M. Agreiter, and B. Stockl. "Revision Rates after Total Joint Replacement." *The Bone and Joint Journal* 93.3 (2011): n. pag. Web.
5. Ryan G, Pandit A, Apatsidis DP. Fabrication methods of porous metals for use in orthopedic applications. *Biomaterials* 2006;27(13):2651.
6. M. Tissakht, H. Eskandari and A. M. Ahmed. Micromotion analysis of the fixation of total knee tibia component
7. E.P. Lautenschlager, P.M., Titanium and titanium alloys as dental materials. *International dental journal*, 1993. 43(3): p. 245-253
8. Elias CN, L.J., Valiev R, Meyers MA, Biomedical applications of titanium and its alloys. *JOM*, 2008. 60(3): p. 46-49
9. O. Okuno, H.H., *Dent. Jpn.*, 1989. 26: p. 101-104
10. G. Cunin, H.B., H. Petite, C. Blanchat, G. Guillemin, *Experimental vertebroplasty using osteoconductive granular material*. *Spine*, 2000. **25**(9): p. 1070-1076
11. J.X. Lu, Z.W.H., P. Tropiano., *Human biological reactions at the interface between bone tissue and polymethylmethacrylate cement*. *J Mater Sci Mater Med*, 2002. **13**(8): p. 803-809

12. J.E. Barralet, T.G., A.J. Wright, I.R. Gibson, J.C. Knowles, *Effect of porosity by compaction on compressive strength and microstructure of calcium phosphate cement*. J Biomed Mater Res (Appl Biomater), 2002. **63**(1): p. 1-9
13. Travan A, Marsich E, Donati I, et al. Polysaccharide-coated thermosets for orthopedic applications: From material characterization to in vivo tests. Biomacromolecules. 2012;13(5):1564-1572
14. Mann KA, Mocarski R, Damron LA, Allen MJ, Ayers DC. Mixed-mode failure response of the cement–bone interface. Journal of Orthopaedic Research. 2001;19(6):1153-1161
15. Lennon AB, McCormack BAO, Prendergast PJ. The relationship between cement fatigue damage and implant surface finish in proximal femoral prostheses. Medical Engineering and Physics. 2003;25(Compendex):833-841
16. McCormack BAO, Prendergast PJ. Microdamage accumulation in the cement layer of hip replacements under flexural loading. Journal of Biomechanics. 1999;32(5):467-475
17. Khandaker M, Riahinezhad S, Inventors. Method and apparatus to coat a metal implant with an extracellular matrix made with electrospun fiber. USA patent no. US9809906 B2, Nov 7, 2017
18. Khandaker M, Riahinezhad S, Inventors. Method and apparatus to control the heterogeneous flow of bone cement and improve osseointegration of cemented implant. August 11, 2016
19. Khandaker M, Snow P, Inventors; University of Central Oklahoma, assignee. Method and apparatus for controlled alignment and deposition of branched electrospun fiber. US patent no. US9359694, Int. Patent no. AD01D500FI, 2016

20. Khandaker M, Riahinezhad S, Sultana F, et al. Effect of collagen- polycaprolactone extracellular matrix on the in vitro cytocompatibility and in vivo bone responses of titanium. *Journal of Medical and Biological Engineering*. 2017;38:1-14
21. Martínez-Calderon M, Manso-Silván M, Rodríguez A, et al. Surface micro- and nano-texturing of stainless steel by femtosecond laser for the control of cell migration. *Scientific Reports*. 2016;6:36296
22. Smeets R, Stadlinger B, Schwarz F, et al. Impact of Dental Implant Surface Modifications on Osseointegration. *BioMed Research International*. 2016;2016:6285620
23. Qiao H, Zhao J, Gao Y. Experimental investigation of laser peening on TiAl alloy microstructure and properties. *Chinese Journal of Aeronautics*. 2015;28(2):609-616
24. Zankovych S, Diefenbeck M, Bossert J, et al. The effect of polyelectrolyte multilayer coated titanium alloy surfaces on implant anchorage in rats. *Acta Biomaterialia*. 2013;9(1):4926-4934
25. Jan Nadorf, Stefan Kinkel, Simone Gantz, Eike Jakubowitz, J. Philippe Kretzer. Tibial revision knee arthroplasty with metaphyseal sleeves: The effect of stems on implant fixation and bone flexibility
26. Khandaker M, Hossan M. Effect of laser texturing and plasma nitriding on titanium. Paper presented at: 2018 ASME congress and exposition 2018
27. Penrose J.M.T. Development of an accurate three dimensional finite element knee model. *Comp. Meth. In Biomech. and Biomed. Eng.* 5:291-300, 2002.
28. Donahue T.L H. et al. A finite element model of the Human knee joint for the study of tibio-femoral contact. *J. Biomech. Eng.* 124:279-280, 2002

29. Beillas P. et al. A new method to investigate in vivo knee behavior using a finite element model of the lower limb. *J Biomech.* 37:019-1030, 2004.
30. Louis E. DeFrate, Hao Sun, Thomas J. Gill, Harry E. Rubash, Guoan Li.” In vivo tibiofemoral contact analysis using 3D MRI-based knee models”, *Journal of Biomechanics*, 37, 1499-1504, 2004
31. Jason P. Halloran, Anthony J. Petrella, Paul J. Rullkoetter. “Explicit finite element modeling of total knee replacement mechanics”, *Journal of Biomechanics*, 38, 323-331, 2005
32. <https://www.element.com/more-sectors/medical-device/knee-implant-testing>
33. Castro, A.P.G., Completo, A., Simões, J.A., Flores, P., Biomechanical behaviour of cancellous bone on patellofemoral arthroplasty with Journey prosthesis: a finite element study. *Computer Methods in Biomechanics and Biomedical Engineering*, 18(10),1090-1098, 2015.
34. Zach L., Ruzicka P., Konvickova S. and L. Cheze, Stress analysis of knee joint endoprosthesis. *Journal of Biomechanics* 40(S2) XXI ISB Congress, Poster Sessions, July, 2007
35. Haut D.T., Hull M., Rashid M., Jacobs C., A finite element model of the human knee joint for the study of tibio-femoral contact. *J. Biomech. Eng.*, 124:273-280, 2002
36. Villa T., Migliavacca F., Gastaldi D., Colombo M., Pietrabissa R., Contact stresses and fatigue life in a knee prosthesis: comparison between in vitro measurements and computational simulations. *J. Biomech.*, 37:45-53, 2004

37. Ishikawa H., Fujiki H., Yasuda K., Contact analysis of ultrahigh molecular weight polyethylene articular plate in artificial knee joint during gait movement. *Journal of Biomechanical Engineering* 118:377-386, 1996
38. Sathasivam S., Walker P.S., Computer model to predict subsurface damage in tibial inserts of total knees. *Journal of Orthopaedic Research* 16, 564-571, 1998
39. S. David Stulberg, MD , Nitin Goyal, BA, Which Tibial Tray Design Achieves Maximum Coverage and Ideal Rotation: Anatomic, Symmetric, or Asymmetric? An MRI-based study